Supporting Information to

Glycopolymer vesicles with an asymmetric membrane

H. Schlaad,[a]* L. You,[a] R. Sigel,[b] B. Smarsly,[c] M. Heydenreich,[d] A. Mantion,[e] A. Mašić[f]

[a] Max Planck Institute of Colloids and Interfaces, Colloid Chemistry, D-14424 Potsdam. [b] University of Fribourg, Adolphe Merckle Institute, CH-1700 Fribourg. [c] Justus Liebig University Giessen, Institute of Physical Chemistry, D-35392 Giessen. [d] University of Potsdam, Institute of Chemistry, D-14476 Golm. [e] University of Basel, Department of Chemistry, CH-4056 Basel. [f] Max Planck Institute of Colloids and Interfaces, Biomaterials, D-14424 Potsdam.

Glycopolymer synthesis and characterization.

1,2-polybutadiene-block-poly(ethylene oxide)s (PB_{65}-PEO_{212} and PB_{68}-PEO_{34}; PDI = 1.1) were synthesized by a two-step anionic polymerization of 1,3-butadiene and ethylene oxide.[S1] The radical addition of 2,3,4,6-tetra-*O*-acetyl-1-thio-β-D-glucopyranose onto PB-PEO was done with azoisobutyronitrile (AIBN) and irradiation with a UV lamp (Hg, λ_{max} ~ 300 nm) at room temperature.[S2] Deacetylation of the glucose units was done in sodium methoxide/methanol/chloroform solution at room temperature.[S2] Final products were suspended in water and freeze-dried; isolated yields: 92% (**1**) and 88% (**2**).

(S1) J. Justynska, Z. Hordyjewicz, H. Schlaad, *Polymer* **2005**, *46*, 12057.
(S2) L. You, H. Schlaad, *J. Am. Chem. Soc.* **2006**, *128*, 13336.

Table S1. Molecular characteristics of glycosylated 1,2-polybutadiene-*block*-poly(ethylene oxide) copolymers **1** and **2**.

Sample	x[a]	y[a]	Glc units[b]	C=C[c]	$w_{hydrophilic}$[d]	PDI[e]
1	65	212	33	0.06	0.76	1.16
2	68	34	30	0.09	0.58	1.08

[a] Number-average degrees of polymerization of PB (*x*) and PEO (*y*), as determined by SEC/NMR. [b] Average number of glucose units attached to the PB segment, as determined by elemental analysis (S/C). [c] Fraction of unreacted double bonds, as determined by NMR. [d] Weight fraction of hydrophilic glucose and PEO [e] Apparent polydispersity index of the protected (acetylated) glycopolymer, as determined by SEC (eluent: THF).

C/H/N/S-specific Elemental Analysis was done with a Vario EL Elemental Analyzer. ^{1}H NMR spectra were recorded at room temperature using a Bruker DPX-400 or Bruker Avance 500 spectrometer. Fourier-transform infrared (FT-IR) spectroscopy was done at room temperature with a BioRad 6000 FT-IR spectrometer equipped with a Single Reflection Diamond ATR. Size exclusion chromatography (SEC) with simultaneous UV and RI detection was performed in chloroform at 25 °C using a column set of two 300 x 8 mm^2 MZ-SD*plus* (spherical polystyrene particles with an average diameter of 5 μm) columns with pore sizes of 10^3 and 10^6 Å. Calibration was done with commercial polystyrene standards.

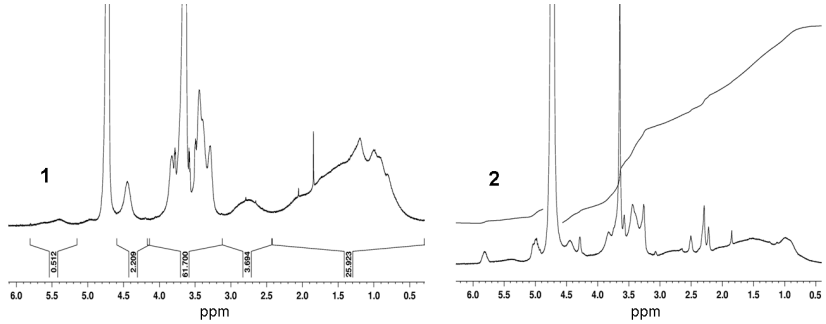

Figure S1. ^{1}H NMR spectra (500.17 MHz) of glycopolymers **1** and **2** in D_2O at room temperature.

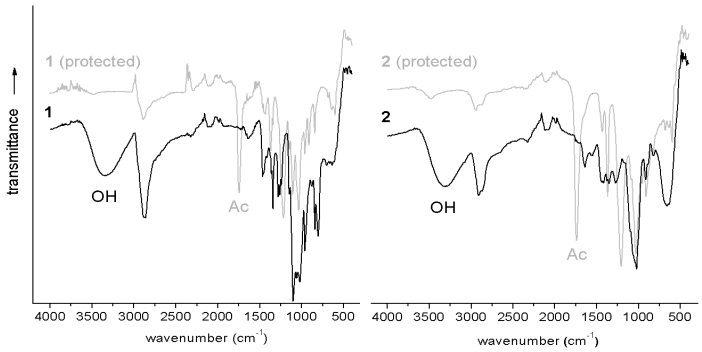

Figure S2. FT-IR spectra of glycopolymers **1** and **2**. The successful removal of acetyl (Ac) protecting groups is indicated by the complete disappearance of the C=O vibration at 1738 cm^{-1} and appearance of the OH vibration at ~3300 cm^{-1}.

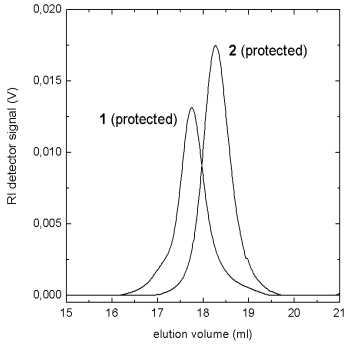

Figure S3. SEC chromatograms of protected glycopolymers **1** and **2** in THF.

Characterization of dilute aqueous solutions of glycopolymers.

Combined static and dynamic light scattering (SLS/DLS) measurements were carried out at 25 °C with a helium-neon laser light source (λ_0 = 633 nm, intensity: 34 mW, Polytec PL3000), an ALV goniometer, and an ALV-5000 multiple-tau digital correlator (ALV GmbH, Langen, Germany). Measurements were performed with 0.025-0.1 wt % polymer solutions (filtered through 5 µm filters, Schleicher-Schüll) at scattering angles from 12°-150° (**1**) or 20°-150° (**2**). Refractive index increments dn/dc = 0.1890 ml/g (**1**) and 0.2131 ml/g (**2**) were measured using an NFT-Scanref differential refractometer operating at λ = 633 nm. For sample **2**, DLS revealed a bimodal size distribution, with small particles of hydrodynamic radius R_h = 14nm and larger aggregates. Their weightings in the correlation function were used as a mean to extract the intensity contribution of the aggregates, which subsequently was treated as SLS data. Since, however, the concentration contribution of the aggregates is unknown, only the radius of gyration R_g and a not very sharp lower limit for the molecular weight M_w can be extracted for this case. The extrapolation of SLS data to the value 0 of the squared scattering vector q^2 was performed in a Berry plot, where only a small curvature is present in the data (Figure S4). Because of the large size of the scattering objects the extrapolation is difficult, and the obtained values M_w = (5±1) 10^9g/mol, R_g = (550±20) nm (**1**) and $M_w >> 4\cdot10^7$g/mol, R_g = (270±40) nm (**2**) are only estimates. The Zimm plots of SLS data show the up-turn characteristic for spherical objects (Figure S5). For **2**, the result for R_g = (250±30)nm from the Zimm plot coincides within the errors with the value from the Berry plot. For **1**, an evaluation of the Zimm plot was not possible. At large q, the intensity follows a q^2-dependency for **2**, which is expected for polydisperse vesicles. For **1**, the intensity shows rather a q^3 behavior at large q. It is most probably caused by form factor effects. The polydispersity is significantly lower than for **2**, as concluded from DLS (see below). In this case, the formfactor is not averaged out.

The evaluation of DLS data was based on the CONTIN software,[S3] which yields the relaxation time distribution. The reduction to the relaxation rate τ_i^{-1} which is equivalent to the initial slope, was performed as described in ref.[S4]. The apparent diffusion constant $D_{app} = \tau_i^{-1}q^{-2}$ was extrapolated to q^2 = 0 (Figure S6) to obtain the true diffusion constant D and the hydrodynamic radius R_h = (520±20) nm (**1**) and R_h = (280±30) nm (**2**). For finite q, the width σ of the relaxation time distribution is affected by particle softness. The effect from the particle size distribution alone is obtained from an extrapolation of σ data to q^2 = 0, similar to a Zimm plot. As a result, $\sigma(q^2=0)$ = 0.6 (**1**) and $\sigma(q^2=0)$ = 1.1 (**2**), i.e. the polydispersity of sample **2** is significantly larger compared to that of **1**. Of further interest is the slope of D_{app} at q^2 = 0, which is expressed as CR_g^2.[S5] With R_g from SLS, the parameter C can be determined. It reflects the polydispersity and softness of the particles. The value C = 0.04 (**1**) and C = 0.11 (**2**) is comparable to our previous results (C = 0.06) for vesicles with polymer chains located within the vesicular shell.[S4] This significant particle softness gives further support for the suggested structure with a very thin vesicular shell, where the higher C value of sample **2** can be understood as a consequence of higher flexibility due to the shorter poly(ethylene oxide) (PEO) chain and higher polydispersity. For vesicles composed of bilayers of an amphiphilic block copolymer, in contrast, a much smaller particle softness (C = 0.005) was found.[S6]

(S3) S. W. Provencher, *Comput. Phys. Commun.* **1982**, *27*, 213-227; ibid, 229-242.
(S4) Z. Hordyjewicz-Baran, L.C. You, B. Smarsly, R. Sigel, H. Schlaad, *Macromolecules* **2007**, *40*, 3901-3903.
(S5) M. Schmidt in *Dynamic Light Scattering*, W. Brown (Editor), Clarendon: Oxford 1993, pp. 372-406.
(S6) R. Sigel, M. Łosik, H. Schlaad, *Langmuir* 2007, *23*, 7196-7199.

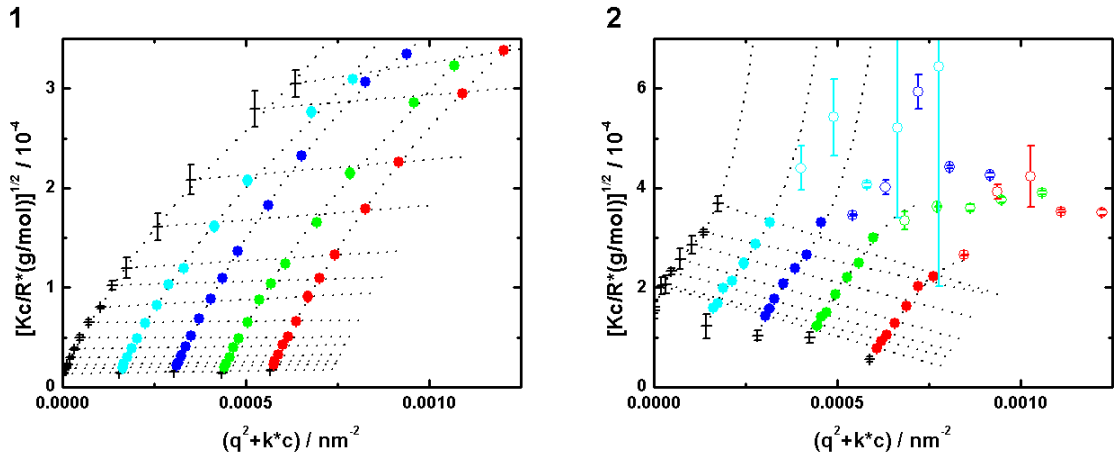

Figure S4. Berry plots of SLS data of dilute aqueous solutions of glycopolymers **1** and **2**. For **2**, only the intensity contribution of the aggregates is considered.

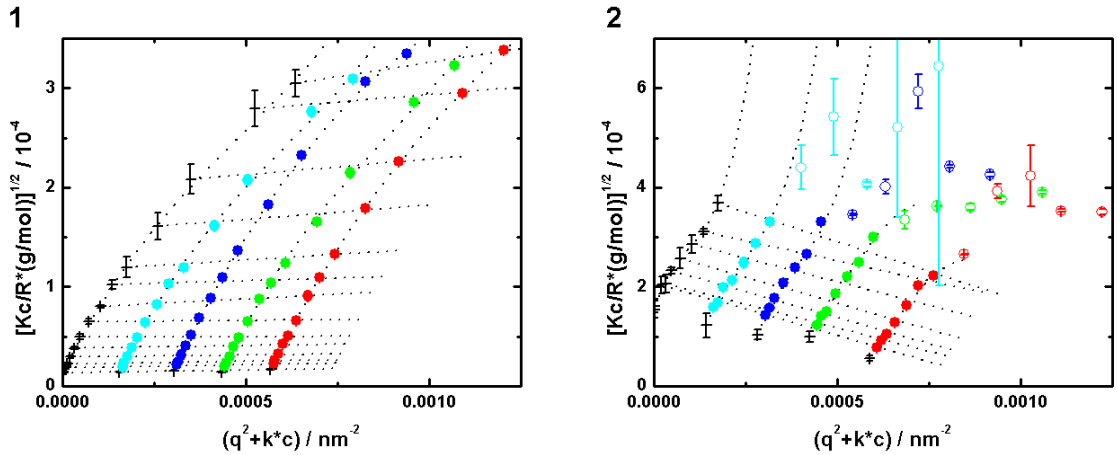

Figure S5. Zimm plots of SLS data of dilute aqueous solutions of glycopolymers **1** and **2**. For **2**, only the intensity contribution of the aggregates is considered.

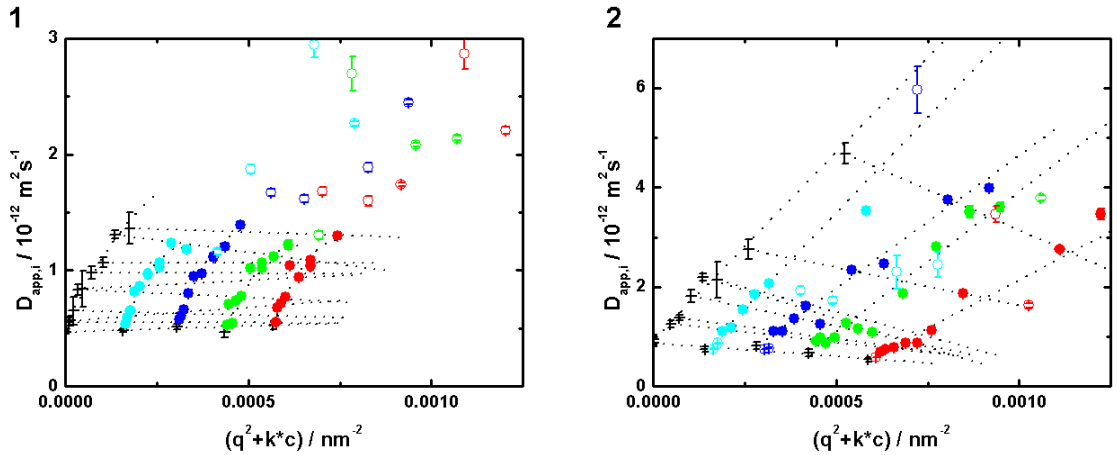

Figure S6. "Dynamic Zimm plots" of DLS data of dilute aqueous solutions of glycopolymers **1** and **2**.

Small-angle X-ray scattering (SAXS) was performed on a polymer solutions in a capillary of Boron-silicates. SAXS data were acquired using a rotating anode (Cu K_α, λ = 0.154 nm) instrument with pinhole collimation at room temperature. The samples were placed at a distance of 1.05 m to a 2 MAR CCD detector. 2D diffraction patterns were transformed into a 1D radial average of the scattering intensity.

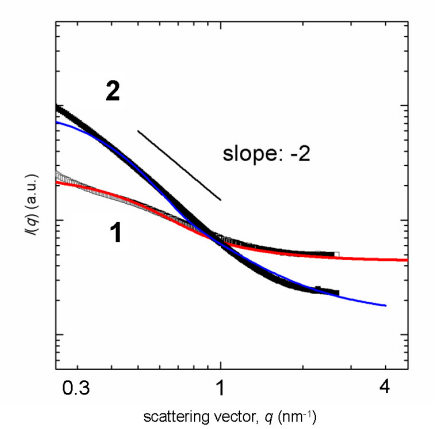

Figure S7. SAXS curves of 10 wt % aqueous solutions of glycopolymers **1** and **2** at room temperature.

The SAXS curves of samples **1** and **2** (Figure S7) were taken at scattering vectors $q > 0.1$ nm^{-1} and are characterized by a shape without distinct features. However, the shape is in agreement with unilamellar vesicles, since the slope in a log-log-plot (ca. -2) is in agreement with hollow objects with a thin membrane. The data were modelled by the approach of Burger and Förster,[S7] assuming vesicles with a diameter being significantly larger than the average membrane thickness. The experimental SAXS data are thus mainly determined by the structural features of the membrane, but not of the vesicles themselves, which would be visible at substantially smaller scattering vectors. Using the approach of Burger and Förster, fitting parameters were the average membrane thickness d, its variance (assuming a Gamma distribution) and the interfacial width d_z between the membrane and surrounding solvent. We obtain for **1** an average membrane thickness of d = 4 nm, a variance of 10% and d_z = 1.5 nm. For **2**, it is d = 5 nm with a variance of ca. 15% and d_z = 0.5 nm. The average thicknesses of the membranes are similar, but the two samples differ significantly in the interfacial width between the membrane core and the surrounding. This finding is reasonable taking into account that sample **1** possesses a longer PEO chain, which leads to a more diffuse transition of electron density between the membrane core and the surrounding.

(S7) Förster, S.; Burger, C. *Macromolecules* **1998**, *31*, 879.

2D-^{1}H,^{1}H-NOESY-NMR spectra (Figure S8) were recorded at room temperature with a Bruker Avance 500 spectrometer operating at 500.17 MHz. Spectra were measured with 48 scans and a mixing time of 150 ms. The Bruker standard Software package was used for acquisition (XWIN-NMR 3.5) and processing (TopSpin 1.3) of data.

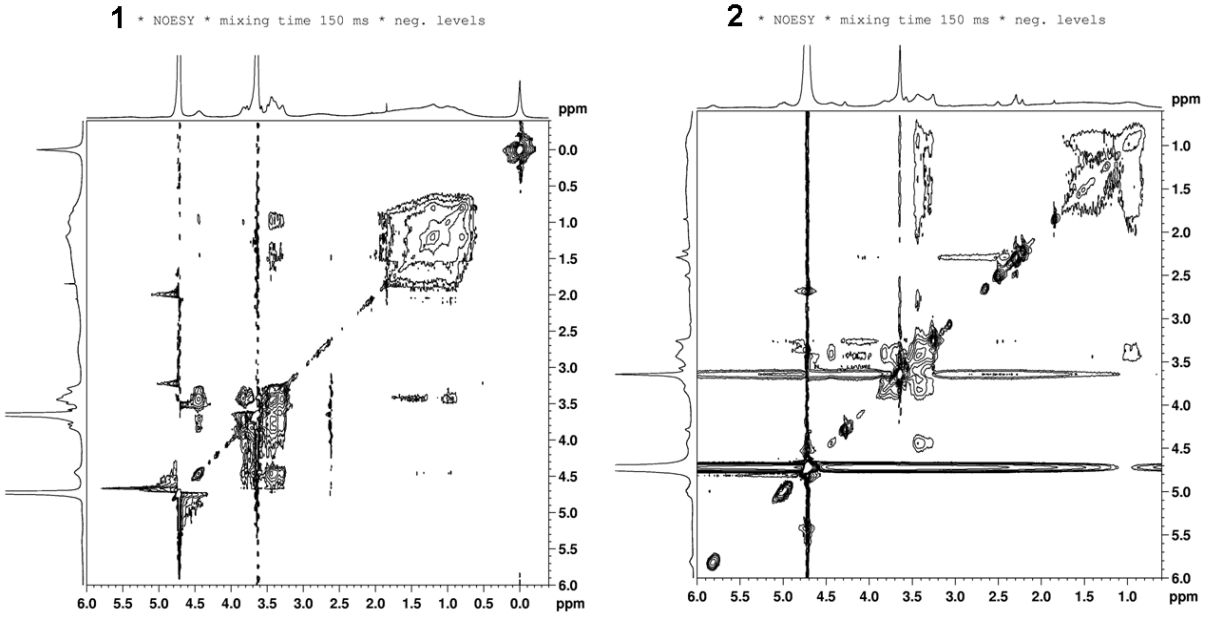

Figure S8. 2D-^{1}H,^{1}H-NOESY NMR (500 MHz) spectra of aqueous solutions of glycopolymers **1** (5.0 mg in 0.5 ml D_2O) and **2** (3.7 mg in 0.5 ml D_2O) at room temperature.

For Raman spectroscopy, a 532 nm Nd:YAG laser (WITec, Ulm, Germany) beam was focused down to a micrometer size spot on the sample through a confocal Raman microscope (CRM300, WITec, Ulm, Germany) equipped with piezo-scanner (P-500, Physik Instrumente, Karlsruhe, Germany). The spectra were acquired using an air-cooled CCD detector (DU401-BV, Andor, Belfast, UK) behind a grating (600 g mm^{-1}) spectrograph (UHTS 300, WITec, Ulm, Germany). The ScanCtrlSpectroscopyPlus (version 1.38, WITec) was used for measurement setup and data processing.
The sample (5 mg polymer in 0.5 ml D_2O, also used for 2D-NMR) was disposed between a microscope slide and a covering object slide and sealed under a slight pressure to stabilize the sample. The sample for SERS was prepared by incubation of 1 equiv. of the polymer solution with 3 equiv. of an aqueous solution of 20 nm gold nanoparticles (Fluka, citrate stabilized).

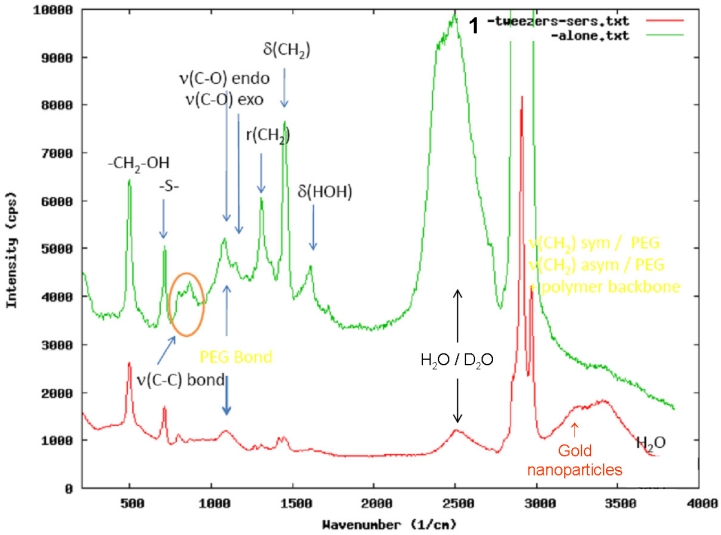

Figure S9. Raman (top) and surface-enhanced Raman (bottom) spectra of the aqueous solutions of glycopolymers **1** (5.0 mg in 0.5 ml D_2O) at room temperature.

The Raman spectrum of the vesicles **1** (Figure S9, green) clearly shows the presence of a thioether ν(C-S) = 717 cm^{-1} at a slightly higher as expected frequency.[S8] All the expected bands for a D-glucose[S9] are present, the aliphatic signals r(CH_2) and the δ(CH_2) at 1316 and 1470 cm^{-1}, and ν(CH_2),sym and ν(CH_2),asym at ~2900 cm^{-1}, and ν(C-H) in CH at ~3000 cm^{-1} (the latter overlapping with the hydrocarbon backbone signals and PEO). The –OH related bands ν(-CH_2-OH) arises at ~500 cm^{-1}, whereas the weak ν(O-H) band expected at 3324 cm^{-1} is not observed.[S8] The bands at 1064 cm^{-1} and 1110 cm^{-1} corresponding to ν(C-O) endo and ν(C-O) exo, respectively, are present. For the PEO residue, one can recognize the w(CH_2-O-CH_2) at ~1100 cm^{-1} (superimposed with sugar signals) and the ν(CH in CH_2),asym and ν(CH in CH_2) at ~2900 cm^{-1}.
For the measurement of the SERS spectrum (Figure S9, red), the solution of vesicles **1** in D_2O were spiked with an aqueous solution of 20 nm sized gold nanoparticles. A signal is observed in SERS when the electric field vector at the nanoparticle surface is collinear with the polarizability vector of a particular bond, which can be used to evaluate which bonds interact with the metallic surface. As can be seen in Figure S9, some bands in the SER spectrum are very repressed, especially those arising from the sugar moiety core. On the other hand, the bands of the PEO chains are not modified or even have become visible. The thioether signal remains at 717 cm^{-1}. The scaling of the both spectra allows us to say that a large part of the C-H related signal vanished, as the alcohol signals, in exception to the ν(CH_2-OH) band at 500 cm^{-1}. The PEO signals remains identical, like the hydrocarbon backbone signals, as evidenced by the ratio ν(CH_2),asym and ν(CH_2),sym. The band at 3250 cm^{-1} cannot be used to further support the adsorption process, as this band is also present in the control experiment with the gold nanoparticle sample alone and are likely caused by the citrate coating.
These results indicate that the gold nanoparticles interact with the glucose units (signals disappear in SERS) and not with the PEO chains (signals remain unchanged). The gold nanoparticles interact with the glucose (thioether) on the outer surface of vesicles and seem not to able to penetrate the membrane and reach the PEO at the inside.

(S8) G. Socrates. *Infrared and Raman characteristic group frequencies*. John Wiley & sons, Chichester, 2001.
(S9) M. Mathlouthi, J. L. Koenig. *Adv. Carbohydr. Chem. Biochem.* **1986**, *44*, 7–89.